ON THE EFFECTS OF TRAILING EDGE BLUNTNESS SIZE OVER AIRFLOW-INDUCED NOISE FOR A NACA0012 AIRFOIL

Behzad Amirsalari [1*] and Joana Rocha [1†]
[1]Department of Mechanical and Aerospace Engineering, Carleton University, Ottawa, ON

1 Introduction

This paper investigates the effects of Trailing Edge (TE) bluntness size on airfoil self-noise using Computational Fluid Dynamics (CFD). The study case is a NACA0012 airfoil with the original chord length (C) of 0.2286m; the airfoil has a varying TE blunted between 0 and 10mm, lowering the effective chord length. The airflow has an Angle of Attack (AoA) of 4° and a free stream velocity of 40m/s. To conduct the CFD simulations, the flow domain consisted of a C-type domain with a length and height of 40C and 10C, respectively. Simulations employ a hybrid Embedded Large-Eddy Simulation (ELES) technique to calculate the flow properties. A correlation length of 0.5C also accounts for spanwise effects in the Ffowcs-Williams and Hawkings (FW-H) acoustic analogy approach to predict far-field noise. Mesh convergence and domain size stability have been checked after verifying the simulation method against available literature [1]. The current study focuses on the relationship between TE bluntness size and Sound Pressure Level (SPL), peak frequencies, and aerodynamic performance of the airfoil.

2 Method

Conventional Reynolds-Averaged Navier-Stokes (RANS) models fall short for capturing flow-induced noise due to their inherent averaging of pressure fluctuations, which are critical for noise calculations. Conversely, employing LES across the entire computational domain is deemed impractical due to its significant computational demands. This study adopts the Embedded LES (ELES) method seeking a balance between accuracy and computational efficiency. This hybridization mitigates computational costs compared to fully resolved LES methods while providing turbulence resolution for aeroacoustic analyses. Here, a relatively smaller computational domain, covering crucial areas such as the downstream portion of the airfoil, TE, and wake zone, is resolved by the LES solver with the SST K-Omega two-equation technique. Meanwhile, the RANS technique models the flow in the remaining areas of the domain.

Considering various parameters, such as flexibility in boundary conditions and compatibility with advanced turbulence models, a C-type domain with 20C and 40C for the width and length, respectively, was designed. This setup involves a standard NACA0012 airfoil with a parameterized blunt TE using 200 points. This parameterization ensures that design and mesh specifications remain independent of the TE size, enhancing the reproducibility and versatility of the simulations. The ELES setup encompasses embedding the LES zone within a URANS domain, facilitated by a RANS-LES interface with a Spectral Synthesis algorithm to synthesize turbulent fluctuations at the boundary [2]. This algorithm decomposes the velocity field into its Fourier modes using a Fast Fourier Transform (FFT), yielding the velocity field in terms of its spatial frequencies. Then, it assigns random phases to each Fourier mode to represent the random nature of turbulence and transforms it back to physical space using the inverse FFT [3]. This synthesized velocity field plays as the boundary perturbations with real-time communication between RANS and LES domains, ensuring seamless integration between RANS and LES.

Although structured face mesh seems to be more stable in the results, unwanted high aspect ratio and very low Courant-Friedrichs-Lewy (CFL) number [4] are some of the critical parameters in using them, favouring a free quad mesh with an inflation layer that fully covers the turbulent boundary layer thickness (Figure 1).

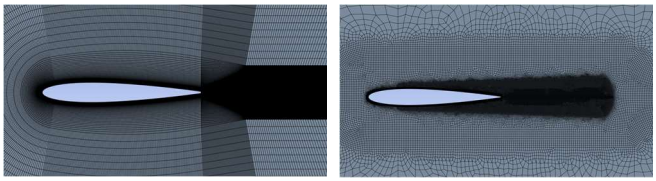

a B

Figure 1: Mesh configuration a) structured, b) unstructured.

This mesh configuration offers better adaptivity to the TE shape and reduces computation time compared to other mesh types. Furthermore, a mesh convergence study was also conducted to enhance the mesh design with respect to the number of perpendicular number of cells in the inflation layer (N), geometric growth rate (G), and the height of the first layer (Y_H) (refer to Table 2).

Table 1: Mesh convergence study

Mesh	elements	N	G	Y_H (E-05)	C_d
1	11912	-	-	-	0.16
2	21290	20	1.3	1.65	0.057
3	29357	25	1.2	1.65	0.053
4	74468	30	1.15	1.65	0.052

The aeroacoustic setup also involves the FW-H analogy (Equation 1) to calculate the pressure-time data at three virtual receivers near the airfoil [1]. The FFT algorithm converts this data from the time domain to the frequency domain, enabling analysis of frequency distribution. This far-field noise output is typically represented as amplitude versus frequency, processed to obtain SPL versus frequency data.

* behzadamirsalari@cmail.carleton.ca
† joanarocha@cunet.carleton.ca

$$\frac{1}{a_0^2}\frac{\partial^2 p'}{\partial t^2} - \nabla^2 p' = \frac{\partial^2}{\partial_{x_i}\partial_{x_j}}\{T_{ij}H(f)\} - \frac{\partial}{\partial_{x_i}}\{[P_{ij} + \rho u_i(u_n - v_n)]\delta(f)\} + \frac{\partial}{\partial t}\{[\rho_0 v_n + +\rho(u_n - v_n)]\delta(f)\} \quad (1)$$

3 Results

Figure 2 shows the SPL results at the mentioned three receivers for the airfoil with 5mm of blunt TE. The influence of bluntness size on aerodynamic and aeroacoustic parameters, i.e. the Cl/Cd ratio, von Kármán vortex street, peak frequency, and SPL for M1 microphone was also investigated, using six different blunt TE sizes between 1mm to 12mm (Table 1). The velocity contours in Figure 3 show the effect of bluntness size on the width of the von Kármán vortex street.

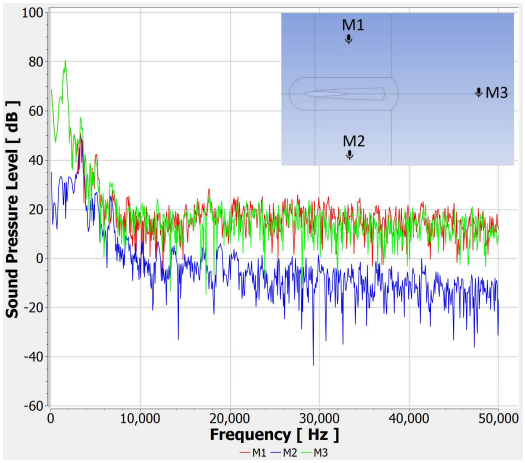

Figure 2: SPL at the three receivers around the TE

Table 2: Aerodynamic and aeroacoustic responses to TE size

TE size	Aerodynamics			Aeroacoustics	
	Cl	Cd	Cl/Cd	Peak freq.	SPL
1 mm	3.34	0.15	21.63	68 Hz	67 dB
2 mm	3.36	0.15	22.56	70 Hz	32 dB
5 mm	2.90	0.14	20.23	1625 Hz	82 dB
8 mm	2.63	0.17	15.47	2220 Hz	63 dB
10 mm	2.36	0.23	10.35	1875 Hz	64 dB
12 mm	2.41	0.27	9.03	765 Hz	85 dB

4 Discussion and Conclusion

The simulations confirm the claims, showing that increasing the bluntness size of an airfoil not only leads to wider von Kármán vortex street but also reduces the aerodynamic efficiency of the airfoil [5]. Data suggests that bluntness effects become noticeable after a size of 5mm (~0.02C), characterized by vortex shedding in the wake region behind the TE. Airfoils with smaller bluntness sizes behave more like sharp TEs, producing lower peak frequency and SPL. Initially, increasing bluntness size shifts peak frequency towards higher frequencies, then back to lower frequencies, which is also confirmed by other references [6, 7]. These impacts are minimal for low bluntness sizes but significant for moderate to larger sizes. However, generally, increasing TE bluntness

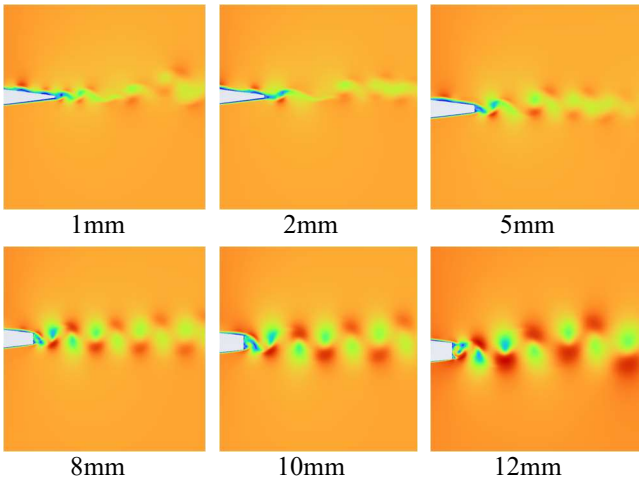

Figure 3: Velocity and von Kármán responses to TE size

size causes an increase in SPL due to turbulent flows with larger eddy shedding [8] and more acoustic energy [9]. As the size and intensity of shedding vortices increase behind the airfoil, it is expected that the SPL from quadrupole sources will also increase [10]. Regarding sound propagation, the microphone placed along the chord line records lower SPL, potentially due to various interference effects such as chord line cancellation and dipole source effect. However, the study notes limitations in the ability of 2D simulations to cover all noise sources comprehensively.

References

[1] Abdessemed, C., A. Bouferrouk, and Y. Yao. Aerodynamic and aeroacoustic analysis of a harmonically morphing airfoil using dynamic meshing. in Acoustics. 2021. MDPI.

[2] Menter, F., et al., An overview of hybrid RANS–LES models developed for industrial CFD. Applied Sciences, 2021. 11(6): p. 2459.

[3] Shur, M.L., et al., Synthetic turbulence generators for RANS-LES interfaces in zonal simulations of aerodynamic and aeroacoustic problems. Flow, turbulence and combustion, 2014. 93: p. 63-92.

[4] Salama, Y. and J. Rocha, Aeroacoustic Investigation of Trailing-Edge Finlets. Advances in Aerospace Science and Technology, 2022. 7(1): p. 1-24.

[5] Hussain, U., et al. Effect of trailing edge serration on the lift and drag characteristics of NACA0012 airfoil wing. in 35th AIAA applied aerodynamics conference. 2017.

[6] Deuse, M. and R.D. Sandberg. Parametric study of multiple aerofoil self-noise sources using direct noise computation. in 25th AIAA/CEAS Aeroacoustics Conference. 2019.

[7] Kershner, J., J. Jaworski, and T.F. Geyer. Experimental study of trailing-edge bluntness noise reduction by porous plates. in AIAA AVIATION 2023 Forum. 2023.

[8] Xing, Y., et al., Effect of wavy leading edges on airfoil trailing-edge bluntness noise. Aerospace, 2023. 10(4): p. 353.

[9] dos Santos, F.L., et al., Wall-pressure spectra, spanwise correlation, and far-field noise measurements of a NACA 0008 airfoil under uniform and turbulent inflows. Applied Acoustics, 2023. 211: p. 109546.

[10] Kojima, Y., et al., On the origin of quadrupole sound from a two-dimensional aerofoil trailing edge. Journal of Fluid Mechanics, 2023. 958: p. A3.